Journal of Solid Mechanics and Materials Engineering

Vol. 2, No. 6, 2008

Mechanical and High Temperature Oxidation Properties of Cold Sprayed CoNiCrAlY Coatings for Thermal Barrier Coating*

Takahiro NIKI**, Kazuhiro OGAWA** and Tetsuo SHOJI**

**Fracture and Reliability Research Institute, Tohoku University,
6-6-1, Aoba, Aramaki, Aoba-ku, Sendai, 982-8579, Japan
E-mail: niki.takahiro@rift.mech.tohoku.ac.jp

Abstract

Cold spraying, which is one of the spraying systems for particle deposition, has been studied as a new system of bond coatings of Thermal Barrier Coatings (TBCs) for components used in hot section of advanced gas turbine systems. In this paper, mechanical and oxidation properties including residual stress of Atmospheric Plasma Sprayed (APS) yttria-stabilized zirconia (YSZ) top coating with two different bond coating spraying systems, Low Pressure Plasma Spraying (LPPS) and the cold spraying, were evaluated and compared in thermal cycle tests. From the results, the porosity of the cold sprayed CoNiCrAlY bond coating is less than 4.2%. The relatively less oxidation layer is observed due to its higher density and more stable oxide growth. In-situ measurement of residual stress in the vicinity of the interface between bond coating and top coating shows that variations of residual stress between the thermal and the cold sprayed coatings are different. In particular, both coatings' residual stresses after thermal cycle test were compression due to oxide formation. The thermal sprayed coating had more oxidation layer than the cold sprayed coating. Therefore, compressive residual stress of the thermal sprayed coating was 40 MPa higher than the cold sprayed coating.

Key words: Cold Spray, Thermal Spray, High Temperature Oxidation, CoNiCrAlY Bond Coating, Residual Stress

1. Introduction

In order to improve the efficiency of gas turbine systems for minimizing the radiation of carbon-dioxide, Thermal Barrier Coatings (TBCs) have been applied to components in hot section of advanced gas turbine systems. Recently, the cold spraying has been studied as a new coating system to apply bond coatings of TBCs. In this system, the coating powder is not melted prior to impingement on the substrate. The conversion of particle's kinetic energy into thermal and strain energies upon striking the substrate leads to a relatively well-adherent and low porosity coating. At low temperature, less than 600°C, coatings are produced with relatively less oxide. Moreover, because of the low temperature, phases presenting the initial powder are retained in the coating. Due to these significant properties, the cold spraying process is considered as a replacement for conventional plasma spraying system. However, details of coating formation mechanism and properties of the cold sprayed TBCs have been unclear.

The aim of this study is to evaluate several properties of TBCs with the cold sprayed bond coatings, such as Vickers hardness, porosity, high temperature oxidation resistance and residual stress.

*Received 16 Nov., 2007 (No. 07-0726)
[DOI: 10.1299/jmmp.2.739]

2. Experimental procedure

2·1 Materials and spray condition

A TBC bond coating of 37.5Co-32Ni-22Cr-8Al-0.5Y was sprayed by cold spraying on a nickel based superalloy (Inconel 601) substrate. The cold spraying equipment used in this study is the high pressure cold spraying system (Inovati KM-CDS 2.1). The thicknesses of the coatings were 80μm, 200μm and 500μm. Fig. 1 shows the TBCs used for each test. The results of porosity, oxidation resistance and residual stress of the cold sprayed coatings were compared to those of the Low Pressure Plasma Sprayed (LPPS) coating. Spray conditions of the LPPS and Atmospheric Plasma Spray (APS) are described in Table 1. All coatings were fabricated by some companies. Therefore, vacuum level and used gun etc. were not clear. Plasma sprayed particles size of CoNiCrAlY and yttria-stabilized zirconia (YSZ) were 5-37 and 11-125 μm, respectively.

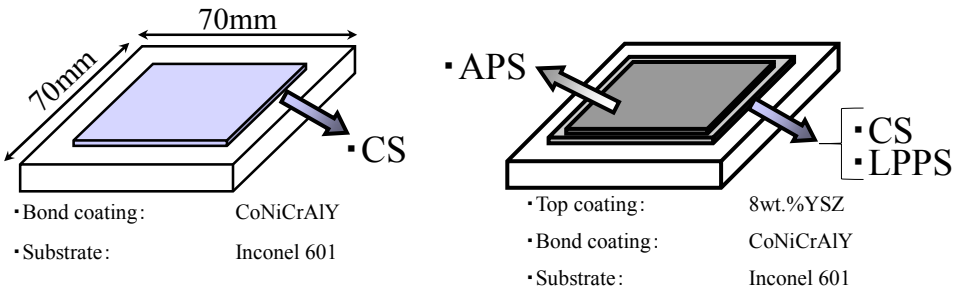

a) Schematic of the specimen of Vickers hardness, porosity and oxidation resistance measurement experiments.

b) Schematic of the specimen of residual stress analysis. Atmospheric Plasma Sprayed YSZ top coating with two different bond coating spraying system, LPPS and cold spraying.

Fig. 1 Schematic illustration of cross sectional image of used specimens.

Table 1 Spray conditions of the LPPS and the APS

Spray system	Primary Gas	Output (kw)
APS	Ar, H_2	33.0
LPPS		40.0

2·2 Measurements of porosity

Each specimen was polished with emery papers, and was then mirror-polished using a diamond paste with a particle diameter 1 μm. Polished particles were not dropped and did not affect the result. Ten random points on the surface of the cold sprayed bond coating were taken by scanning electron microscope (SEM). Porosity of the bond coating was calculated by using image data processing. Schematic illustration of the porosity measurement is shown in Fig. 2.

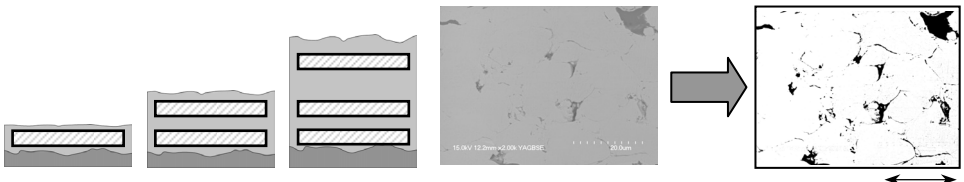

a) Measurement region b) Color calibration of SEM image

Fig. 2 Schematic illustration of the procedure for porosity measurement.

2·3 Measurements of Vickers hardness

Vickers hardness of the bond coating was measured to figure out the sequential hardness distribution. Hardness at ten optional points that have equal distance from a substrate was measured. Applied maximum load and time were 30 mN and 20 sec, respectively. And then, the average values and standard deviation were calculated.

2·4 Evaluation of oxidation resistance

In this study, oxidation resistance of the cold sprayed bond coating was evaluated by observing SEM image of thermally aged surface, and the results were compared with those of the thermal sprayed one. Table 2 shows the heat treatment condition.

Table 2 Heat treatment conditions.

Temperature (^{o}C)	1000
Aging time (hour)	50
	500

2·5 In-situ measurements of residual stress close to the interface between bond coating and top coating

Residual stresses in Atmospheric Plasma Sprayed YSZ top coatings with two different bond coatings produced by thermal and cold spray were evaluated and compared in thermal cycle tests. The furnace used for the tests is shown in Fig. 3. The analyses in which synchrotron orbital radiation for residual stress were performed at the BL02B1 beamline in the SPring-8 synchrotron radiation facility with the approval of the Japan Synchrotron Radiation Research Institute (JASRI). Residual stress determination by using the sin 2ψ method (χ-mode, angle of sample rotation perpendicular to ω- and 2θ-axis) has been taken under consideration. For this purpose the variation of the diffraction angle of the Zr (511) plane reflex was observed. The evaluation formula of residual stress and effective elastic parameter for X-Ray are described in Eqs. 1 and 2[(1)~(2)]. Figure 4, Tables 3 and 4 show the conditions of thermal cycle test and X-ray resolution, respectively.

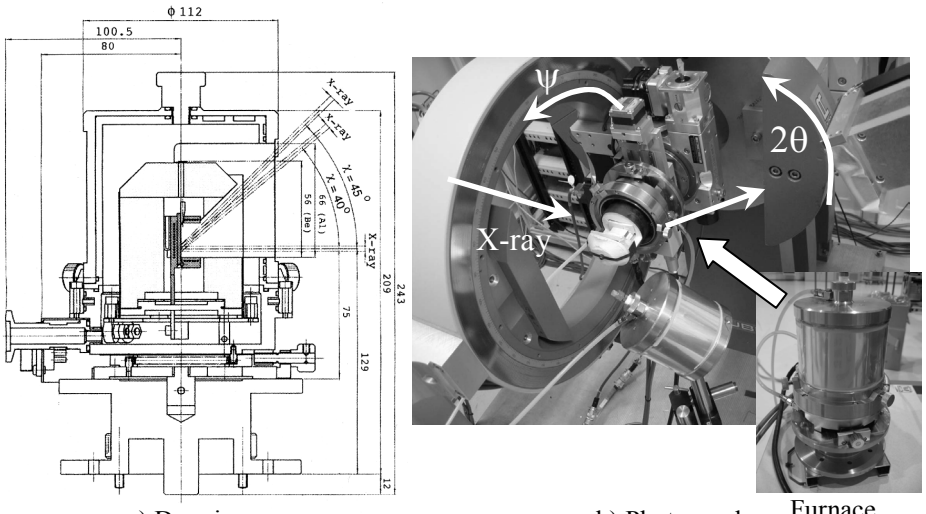

Fig. 3 Drawing and overview of furnace.

$$\sigma_x = -\left\{\frac{E}{2(1+\upsilon)}\right\}\left(\frac{\pi}{180}\right)\cot\theta_0\left\{\frac{\partial(2\theta)}{\partial(\sin^2\psi)}\right\} \quad (1)$$

Effective Elastic Parameter for X-Ray:

$$\frac{E}{2(1+\upsilon)} = 113GPa \quad (2)$$

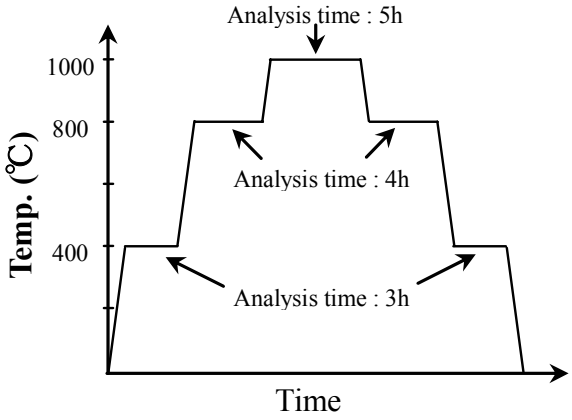

Fig. 4 Thermal cycle pattern.

Table 3 Thermal cycle conditions. It took 30 minutes for temperature stabilization before each measurement.

Temperature increase	Temperature decrease
25→800℃: 2.5℃ / sec.	1000→800℃: 0.6℃ / sec.
800→1000℃: 1.5℃ / sec.	800→400℃: 0.4℃ / sec.
	400→25℃: 0.2℃ / sec.

Table 4 X-ray resolution

Energy range	5 ~ 115 keV
Energy resolution	$\Delta E/E = 10^{-4}$
Photon flux	10^{10} photons/s
Beam size above specimen	3×0.1 mm^2

3. Results and discussion

3·1 Porosity

Fig. 5 shows change in the porosity in terms of distance from surface obtained in specimens that have different coating thicknesses, 80 μm, 200 μm and 500 μm. The average porosity of the thermal sprayed bond coating is approximately 10.5 %, while the porosity of cold sprayed coating is less than 4.2 % regardless of thickness.

By focusing on the relationship between averaged porosity and the distance from surface, decreasing in porosity was noted as the distance increased. This is attributed to the fact that accelerated particles impinged onto the substrate accumulate with continuous impingement. Therefore, upper accelerated particles push lower particles together, for this reason, cavity or porosity in lower layers considerably decreased. Consequently, less porosity was observed due to continuous compressive force applied into the bond coating.

V. Higuera et al.[3] reported that the porosity of the thermal sprayed CoNiCrAlY bond coating is 4.4-5.8 %. This is about half value of the porosity of the thermal sprayed coating measured in this study. Particle diameter and spray conditions of V. Higuera's bond coating and this thermal sprayed coating are almost same. Accuracy of surface finishing and image data processing may affect the result. Porosities of the thermal sprayed coating and the cold sprayed coatings in this study were measured under the same condition.

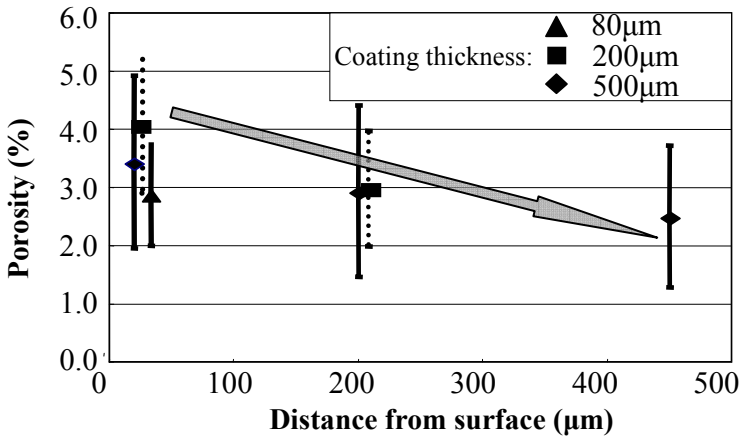

Fig. 5 Relationship between porosity and distance from surface in the cold sprayed CoNiCrAlY.

3·2 Vickers hardness

Average and deviation of Vickers hardness of cold sprayed CoNiCrAlY bond coatings with different coating thicknesses are shown in Fig. 6. The average hardness of 80 μm coating is lower than the other coatings. These results indicate that work hardening by particles' accumulation with continuous impingement is the reason for the low hardness of 80 μm coating.

Values of hardnesses of all coatings with different thicknesses are low near the substrate. It is thought that relatively soft Inconel 601 substrate can affect the hardness of coatings. The hardness of Inconel 601 is approximately 200 HV. On the other hand, hardness of the cold sprayed CoNiCrAlY bond coating is 550-700 HV. By comparing two materials, the cold sprayed CoNiCrAlY has higher hardness than the substrate Inconel 601.

Ranges of standard deviation of hardness in all thickness vary widely. Cavities were avoided in this measurement. However, inner cavities might affect the hardness. And maximum load is 30 mN. In the case of lower loading, hardness value is affected by the condition of cross-sectional indent surface normally, which also affects the hardness value.

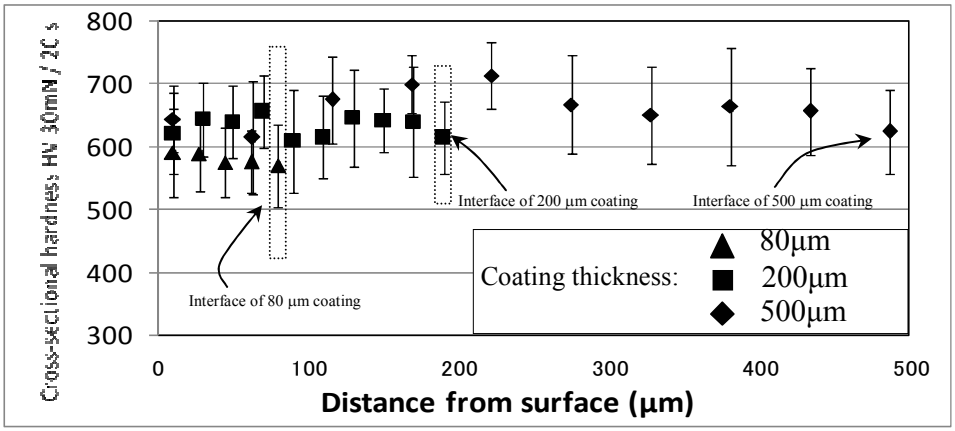

Fig. 6 Comparison of Vickers hardness of bond coatings with different coating thicknesses.

3·3 High temperature oxidation resistance

Figure 7 shows SEM images of the cold sprayed and thermal sprayed bond coatings. From the image of the thermal sprayed bond coating in Fig. 7 (b) - LP, which is 50 hours aged coating, many oxides are observed. By contrast, in the case of the cold sprayed coatings, less oxidation layers are present. The cold sprayed bond coatings have higher density, therefore, oxygen supply through vacancy to the cold sprayed bond coatings is less than the thermal sprayed coating. Oxidation layers of the thermal sprayed coating are higher than standards the thermal sprayed coatings in some degree, though oxidation layers reported by D. Seo[4] et al., and Feng Tang[5] et al. are similar as this the thermal sprayed coatings.

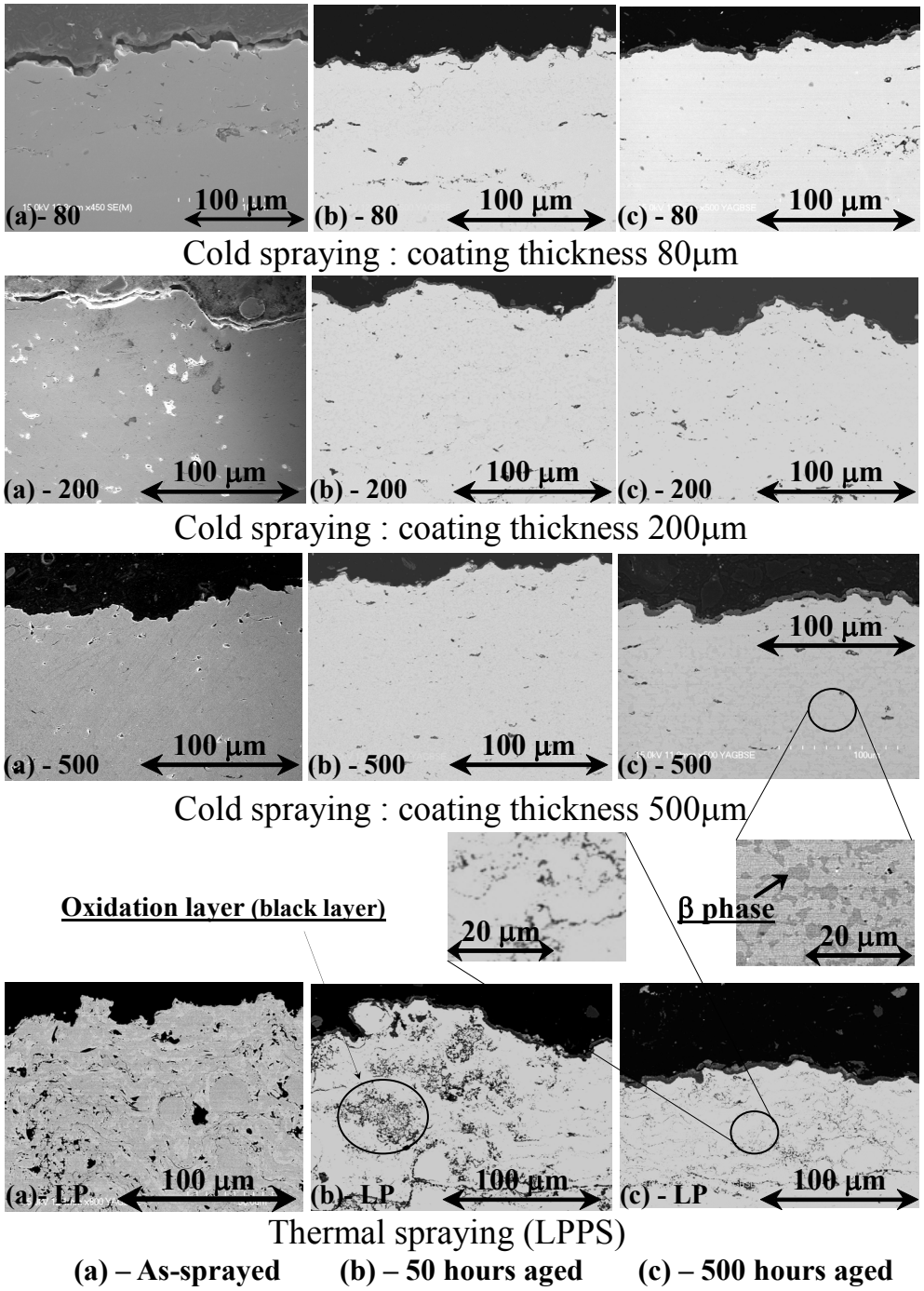

Fig. 6 Comparison of microstructure with different coating thickness and aging hours. (Aging temp. 1000°C)

Generally, rich β phase regions, which are composed of NiAl, are present at as-sprayed and the beginning of thermal aging, and then, that region decreases with increasing aging time due to diffusion of Al to Thermal grown oxide (TGO). From Fig. 7 (c) - 500, a SEM image of the cold sprayed coating with 500 μm thickness and aged for 500 hours, rich β phase regions are easily found. On the other hand, β phase cannot be found in case of the thermal sprayed coating ((c) – LP). The cold sprayed bond coating produces more stable and denser TGO with relatively rapid growth in early stage. Average thickness of TGO in the cold sprayed bond coating is slightly thinner than that of the thermal sprayed one. This result is shown in Fig. 8. The stable and dense TGO can prevent Al diffusion. Accordingly, the cold sprayed coating keeps higher Al concentration than the thermal sprayed one does. Consequently, the cold sprayed bond coating exhibits the properties of higher oxidation resistance.

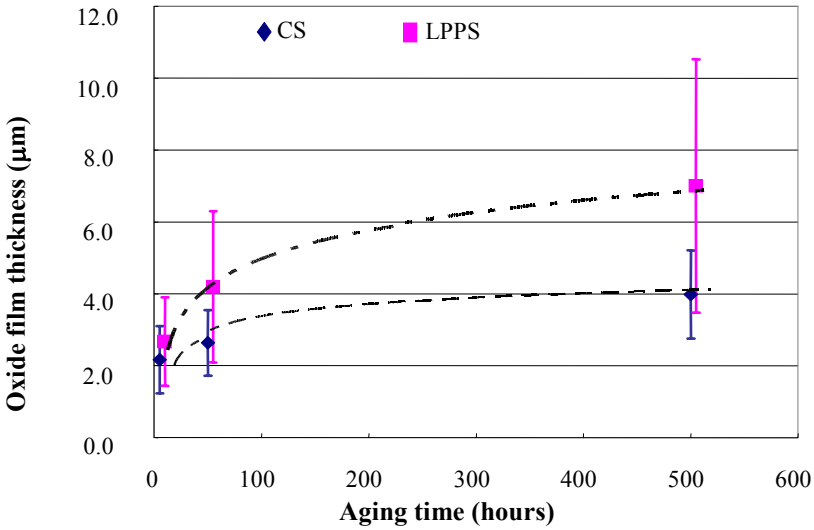

Fig. 7 Comparison of thicknesses of oxidation layer in surfaces of CoNiCrAlY.

3·4 In-situ measurement of residual stress

Residual stress in top coating area was analyzed, which is close to the interface between bond coating and top coating, YSZ. Phase transformation temperature of YSZ is around 1200 °C. Therefore YSZ rarely transforms in this thermal cycle condition and lattice parameter variations indicate residual stress variations. From Fig. 9, in case of the thermal sprayed coating, tensile residual stress was observed at elevated temperature up to 400 °C. Relaxation of the residual stress was promoted beyond 400°C. And then, residual stress drastically transforms to compression after cooling down to 800 °C. In the last thermal cycle test, about 80 MPa compression stress was observed. On the other hand, gradual increase of tensile residual stress was observed up to 1000 °C in case of the cold sprayed bond coating. Moreover, during cooling down, residual stress did not transform to compression until 400 °C. The final difference of each residual stress in thermal cycle test was approximately 40 MPa. Compressive stress caused detrimental effects with respect to delamination[(6)~(7)]. As a result, it is believed that the cold sprayed bond coating, which has lower residual stress, is superior to thermal sprayed bond coating.

Room-temperature residual stress in onset is around 0 MPa (slightly compression). Analyzed depth of residual stress is approximately 200 μm and average values are analyzed in this test. Measured residual stresses were approximately zero, however, they may be balanced out by the value of the YSZ / CoNiCrAlY interface and the surface of YSZ.

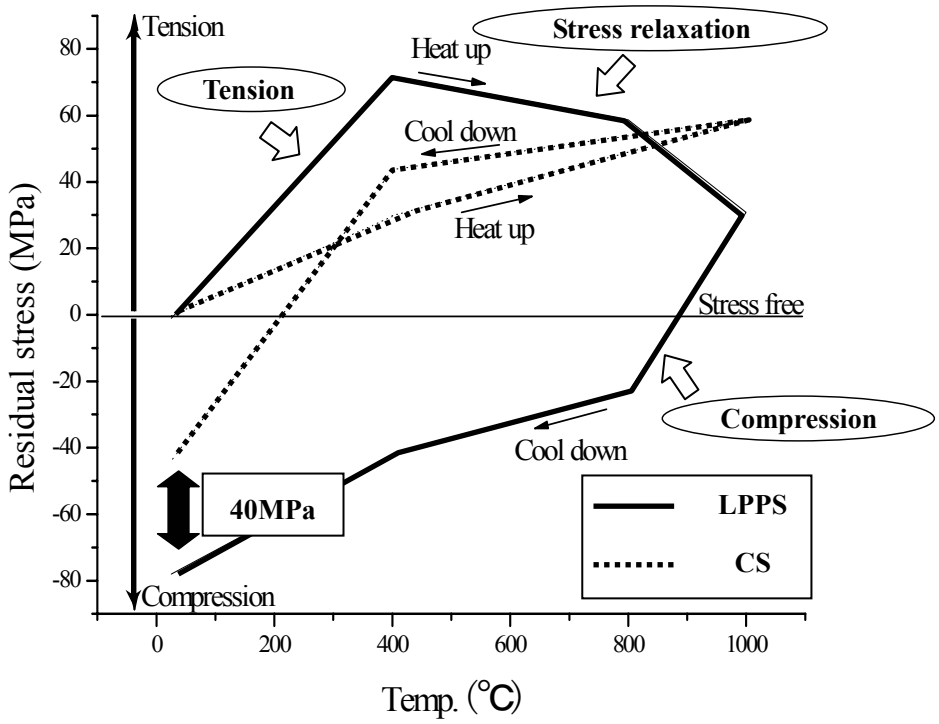

Fig. 8 Variation of residual stresses during thermal cycling tests.

4. Conclusions

In this study, the properties of TBCs with cold and thermal sprayed bond coatings were evaluated by such Vickers hardness, porosity, oxidation resistance and residual stress measurements. From this study, it is concluded that,.

(1) The averaged porosity of the thermal sprayed bond coating is approximately 10.5 %, while porosity sprayed by the cold spraying is less than 4.2 % regardless of thickness in this study. The cold sprayed bond coating is superior to the thermal sprayed coating from the viewpoint of porosity.

(2) The average hardness of 80μm coating is lower than the other two thickness coating. This result indicates due to work hardening by particles accumulation with continuous impingement.

(3) 50 hours aged thermal sprayed bond coating had huge oxidation layers. By contrast, in the case of the cold spraying, less oxidation layers were present. It is believed that the cold sprayed bond coating has a greater density. Therefore, oxygen supplied to the cold sprayed bond coating is less than thermal sprayed one.

(4) From in-situ measurement of residual stress in the vicinity of the interface between bond coating and top coating, variations of residual stress between the thermal sprayed and the cold sprayed coatings are different. In particular, both coatings' residual stresses after thermal cycle test were compression due to oxide formaion. The thermal sprayed coating had more oxidation layer than the cold sprayed coating. Therefore, compressive residual stress of the thermal sprayed coating was 40 MPa higher than the cold sprayed coating. The compressive stress can cause detrimental effects with respect to

delamination. As a result, it is believed that the cold sprayed bond coating, which has lower residual stress, is superior to thermal sprayed bond coating.

References

(1) K. Suzuki, S. Machiya, K. Tanaka and Y. Sakaida, *Transactions of the Japan Society of Mechanical Engineers, Series A*, Vol. 67, No. 660 (2001), pp.1325-1331 (in Japanese).

(2) K. Suzuki, S. Machiya, K. Tanaka and Y. Sakaida, *Transactions of the Japan Society of Mechanical Engineers, Series A*, Vol. 67, No. 655 (2001), pp.417-423 (in Japanese).

(3) V. Higuera, F.J. Belzunce and J. Riba, *Surface & Coatings Technology* , Vol. 200 (2006), pp.5550-5556.

(4) D. Seo, K. Ogawa, M. Tanno, T. Shoji and S. Murata, *Surface and Coatings Technology*, Elsevier Science Ltd., Volume 201, Issue 18, 25 (2007), pp. 7952-7960.

(5) Feng Tang, Leonardo Ajdelsztajn, George E. Kim, Virgil Provenzano and Julie M. Schoenung, *Materials Science and Engineering: A*, Volume 425, Issues 1-2, 15(2006), pp.94-106.

(6) J.S. Wang and A.G. Evans, *Acta Materialia*, Elsevier Science Ltd.,Vol. 47, 2 (1999), pp.699-710.

(7) H.E. Evans, A. Strawbridge, R.A. Carolan and C.B. Ponton, *Materials Science and Engineering A*, Elsevier Science Ltd., Vol. 225, 1-2 (1997), pp.1-8.

Acknowledgments

We are indebted to Dr. S. Kimura at JASRI, Dr. T. Shobu at Japan Atomic Energy Agency and Prof. K. Suzuki, Mr. Y. Kanai and Mr. A. Ohsato at Niigata University for operating the facility and advice on data analysis.

We are indebted to the president Howard Gabel, Inovati for provision of materials under test.

The synchrotron radiation experiments were performed at the beam line, BL02B1 in SPring-8 with the approval of JASRI. (Proposal No. 2006B1361)

This work was supported by a 21st Century COE Program, The Exploration of the Frontiers of Mechanical Science Based on Nanotechnology.